


## ORIGINAL ARTICLE

# Knockdown of long non-coding RNA linc-ITGB1 inhibits cancer stemness and epithelial-mesenchymal transition by reducing the expression of Snail in non-small cell lung cancer

Lili Guo<sup>1,2\*</sup> , Cencen Sun<sup>2\*</sup>, Shilei Xu<sup>1</sup>, Yue Xu<sup>1</sup>, Qiuping Dong<sup>1</sup>, Linlin Zhang<sup>3</sup>, Wei Li<sup>1</sup>, Xingyu Wang<sup>1</sup>, Guoguang Ying<sup>1</sup> & Fengjie Guo<sup>2</sup>

1 Laboratory of Cancer Cell Biology, Tianjin Cancer Research Institute, Tianjin Key Laboratory of Cancer Prevention and Therapy, National Clinical Research Center for Cancer, Tianjin Medical University Cancer Institute and Hospital, Tianjin, China

2 Tianjin Key Laboratory of Lung Cancer Metastasis and Tumor Microenvironment, Tianjin Lung Cancer Institute, Tianjin Medical University General Hospital, Tianjin, China

3 Oncology Department, Tianjin Medical University General Hospital, Tianjin, China

## Keywords

Cancer stem cell; epithelial-mesenchymal transition; linc-ITGB1; non-small cell lung cancer; snail.

## Correspondence

Guoguang Ying, Tianjin Key Laboratory of Cancer Prevention and Therapy, National Clinical Research Center for Cancer, Tianjin Medical University Cancer Institute and Hospital, Huan-Hu-Xi Road, Ti-Yuan-Bei, He-Xi District, Tianjin 300060, China.  
Tel/Fax: +86 22 2351 9721  
Email: yingguoguang163@163.com

\*These authors contributed equally to this work.

Received: 19 September 2018;

Accepted: 10 October 2018.

doi: 10.1111/1759-7714.12911

Thoracic Cancer **10** (2019) 128–136

## Introduction

Lung cancer is the leading cause of cancer-related death worldwide,<sup>1</sup> and non-small cell lung cancer (NSCLC) accounts for approximately 85% of all cases. The main cause of death in patients with lung cancer is tumor metastasis, which can be attributed to multiple factors, such as cancer stem cells (CSCs) and epithelial-mesenchymal transition (EMT). CSCs might be responsible for tumor

initiation and progression, as well as invasion and migration as a result of their capability for self-renewal and potential for proliferation.<sup>2</sup> Many studies have shown that various stemness-related transcription factors, such as *Nanog*, *Oct-4*, *c-Myc*, and *Sox2*, and signaling pathways are involved in the self-renewal of CSC properties of cancer cells.<sup>3</sup> Emerging evidence suggests that EMT plays important roles in the initiation and function of CSCs and

## Abstract

**Background:** The main cause of death in patients with non-small cell lung cancer (NSCLC) is the progression of cancer metastasis, which can be attributed to multiple factors, such as cancer stem cells (CSCs) and epithelial-mesenchymal transition (EMT). Long non-coding RNAs (lncRNAs) play important roles in the regulation of the cell cycle, cell proliferation, immune responses, and metastasis in cancers, but the potential roles and mechanisms of lncRNAs in CSC-like properties of cancer have not yet been elucidated.

**Methods:** Human NSCLC cell lines (A549 and H1299), highly metastatic cell lines (L9981 and 95D), and their corresponding low-metastatic cell lines (NL9980 and 95C) were subject to quantitative real-time PCR and Western blot, transwell invasion, colony formation, and wound healing assays.

**Results:** Linc-ITGB1 was greatly upregulated in CSC spheres. Linc-ITGB1 knockdown markedly inhibited CSC formation and the expression of stemness-associated genes, such as *Sox2*, *Nanog*, *Oct-4*, *c-Myc*, and *CD133*. Depletion of linc-ITGB1 expression also inhibited the in vitro invasive and migratory potential of cells, and further analysis indicated that linc-ITGB1 knockdown increased the expression of the epithelial marker E-cadherin and downregulated the mesenchymal markers vimentin and fibronectin. The EMT-related transcription factor Snail mediated these effects of linc-ITGB1 in NSCLC, and overexpression of Snail significantly reversed the inhibitory effects of linc-ITGB1 depletion.

**Conclusion:** Overall, our study demonstrated that linc-ITGB1 promoted NSCLC cell EMT and cancer stemness by regulating Snail expression.

epithelial cells can gain CSC characteristics through EMT progression.<sup>4</sup>

Cells undergoing EMT often lose typical epithelial characteristics, such as cell polarity and cell-to-cell junctions, and gain a mesenchymal phenotype with increased motility and invasiveness.<sup>5</sup> Loss of expression of the epithelial molecule E-cadherin is considered the main molecular event of EMT, which is also characterized by the expression of mesenchymal markers, such as vimentin, fibronectin,  $\alpha$ -SMA, and  $\beta$ -catenin.<sup>6</sup> EMT-inducing transcription factors, such as Snail, Slug, Zeb1, Zeb2/SIP1, and Twist are activated during EMT and bind to E-boxes in the E-cadherin promoter to repress its transcription.<sup>7</sup>

In addition to the canonical transcriptional programming during EMT, post-transcriptional regulation by microRNAs and non-coding RNAs (lncRNAs) plays an important role in gene regulation during EMT.<sup>8</sup> LncRNAs, a class of non-protein-coding transcripts longer than 200 nucleotides, have emerged as key regulators of a wide range of biological processes, and their abnormal expression is closely associated with tumor proliferation, differentiation, apoptosis and metastasis.<sup>9,10</sup> Several lncRNAs, such as MALAT-1<sup>10,11</sup> and lncRNAH19,<sup>12</sup> are reported to participate in the regulation of EMT. Among the classified subtypes of lncRNA (intergenic, intronic, sense, antisense, and chimeric),<sup>13</sup> long intergenic non-coding RNAs (lincRNAs), whose transcription loci are located between two protein coding genes, have exhibited diverse biological functions in cell cycle regulation, cell proliferation, immune responses, and metastasis in various cancers;<sup>14,15</sup> however, the potential roles and mechanisms of lincRNAs in the CSC-like properties of cancer remain largely unknown.

Linc-ITGB1, a newly discovered lncRNA, has been shown to be involved in the migration and invasion of gallbladder and breast cancer,<sup>16,17</sup> but the expression and function of linc-ITGB1 in lung cancer remains undetermined. Therefore, we conducted this study to clarify the roles and mechanisms of lincRNAs in CSC-like properties of cancer.

## Methods

### Cell culture and lentivirus infection

Human NSCLC cell lines (A549 and H1299), highly metastatic cell lines (L9981 and 95D), and their corresponding low-metastatic cell lines (NL9980 and 95C) were cultured in RPMI-1640 medium supplemented with 10% bovine serum and 1% penicillin/streptomycin (Gibco, Grand Island, NY, USA) at 37°C in a 5% CO<sub>2</sub> incubator. The short hairpin RNA (shRNA) sequence targeting the human linc-ITGB1 gene, 5'-GCAGCTGTTCCAG AATATTGCTCGAGCAATATTCTGGAAACAGCTGC-3', was obtained from a previous study,<sup>16</sup> and the lentivirus

stably expressing the shRNA against linc-ITGB1 was synthesized by Genepharma (Shanghai, China). Briefly, the shRNA was cloned into the lentiviral vector pFH-GFP and the 293T cells were then transfected with the reconstructed vector and two packaging vectors, pCMV $\Delta$ R8.92 and pVSVG-I, to generate the lentivirus. Lentiviral particles (targeting linc-ITGB1: shlinc-ITGB1; or control: shCtrl) were collected from cell supernatants by centrifugation every 48 hours after transfection. For lentivirus infection, cells were seeded into six-well plates ( $5 \times 10^4$  cells/well), infected with the lentivirus at a multiplicity of infection (MOI) of 50, and cultured for 48 to 72 hours.

### Quantitative real-time PCR

Total RNA was isolated from cells using TRIzol reagent (Invitrogen, Carlsbad, CA, USA) according to the manufacturer's instructions and quantified using an ultraviolet spectrophotometer (Beckman Coulter, Fullerton, CA, USA). A total of 2  $\mu$ g of RNA was reverse transcribed using an M-MLV Reverse Transcriptase Kit (Promega, Madison, IL, USA) according to the manufacturer's protocol. The resultant complementary DNA (cDNA) was mixed with ABI SYBR Green Master Mix and primers targeted to the genes of interest and amplified using an ABI7500 Real-time PCR System according to the manufacturer's protocol (Applied Biosystems, Foster City, CA, USA). PCR amplifications were performed in triplicate for each sample. The relative RNA expression was calculated using the  $2^{-\Delta\Delta C_t}$  method. The gene-specific primer sequences are listed in Table 1.

### Cell transfection

Briefly,  $\sim 10^6$  cells were cultured in a six-well plate the day before transfection. Cell transfections were performed using Lipofectamine 2000 (Invitrogen) with 4  $\mu$ g of a plasmid containing the Snail cDNA sequence, and the cells were collected for assays after 72 hours.

### Western blot assay

Cells with the indicated treatments were collected and lysed with complete cell lysis buffer (Beyotime Biotechnology, Shanghai, China) containing a protease inhibitor cocktail (Roche, Basel, Switzerland). For each sample, 40–80  $\mu$ g of total protein was loaded and separated on sodium dodecyl sulfate polyacrylamide gel and transferred to a nitrocellulose (NC) membrane (GE Healthcare, Piscataway, NJ, USA). The membranes were blocked in 5% non-fat milk at room temperature for one hour and incubated overnight at 4°C with primary antibodies targeting E-cadherin (Invitrogen); Vimentin,  $\beta$ -actin (Sigma-Aldrich, St Louis, MO, USA); Fibronectin

**Table 1** Sequences of real-time PCR primers

Gene	Primer	Sequence(5'-3')
linc-ITGB1	Forward	CCTCTCAGCCTCCAGCGTTG
	Reverse	TGCTCTTGCTCACTCACACTCC
E-cadherin	Forward	AGAACGCATTGCCACATACACTC
	Reverse	CATTCTGATCGGTTACCGTGATC
Fibronectin	Forward	AAACCAATTCTTGGAGCAGG
	Reverse	CCATAAAGGGCAACCAAGAG
Vimentin	Forward	GCAAAGATTCCACTTTGCGT
	Reverse	GAAATTGCAGGAGGAGATGC
Snail	Forward	TTACCTTCCAGCAGCCCTA
	Reverse	CCCACTGTCCTCATCTGACA
Slug	Forward	GGGGAGAAGCCTTTTCTTG
	Reverse	TCCTCATGTTTGTGAGGAG
Twist	Forward	GTGCGCAGTCTTACGAGGAG
	Reverse	GCTTGAGGGTCAGAATCTTGCT
Oct4	Forward	CTGCAGTGTGGGTTTCGGGCA
	Reverse	CTTGCTGCAGAAAGTGGGTGGAGGAA
Nanog	Forward	CATGAGTGTGGATCCAGCTTG
	Reverse	CCTGAATAAGCAGATCCATGG
Sox2	Forward	CATCACCCACAGCAAATGACAGC
	Reverse	TTGCGTGAGTGTGGATGGGATTG
c-Myc	Forward	TTCTCTCCGTCCTCGGATTCTCTG
	Reverse	TCTTCTTGTCTCTCAGAGTCG
CD133	Forward	TGATGTCAGAACTTGACAACTG
	Reverse	ATACCTGCTACGACAGTCGTGGT
GAPDH	Forward	CATCACCATCTTCCAGGAGCG
	Reverse	TGACCTTGCCCACAGCCTT

GAPDH, glyceraldehyde 3-phosphate dehydrogenase.

(Abcam, Cambridge, UK); Snail, Slug, Twist, Sox2, Nanog, c-Myc (Cell Signaling Technology, Danvers, MA, USA); and Oct4 (Saiarbio, Beijing, China). The membranes were washed three times for five minutes with Tris-buffered saline with Tween-20 (TBST) and then incubated with an anti-mouse or anti-rabbit horseradish peroxidase-conjugated secondary antibody (Cell Signaling Technology) for 60 minutes at room temperature. Protein signals were visualized by incubating the membrane with a chemiluminescent horseradish peroxidase substrate (Millipore, Billerica, MA, USA), and the film was developed in a medical X-ray processor (Eastman Kodak Company, Rochester, NY, USA).

### Transwell invasion assay

Cell migration and invasion assays were conducted using Biocoat Matrigel Invasion Chambers (BD Biosciences) according to the manufacturer's recommended instructions. In brief, cells ( $4 \times 10^4$ ) were plated in the upper chamber in 200  $\mu$ L of serum-free medium. Dulbecco's modified Eagle medium with 10% fetal bovine serum was added to the bottom chamber as a chemoattractant to induce cell invasion, and the plate was incubated for 24 hours at 37°C. The non-migrating cells were then removed from the upper part of

the filter using a cotton swab. The transwell membranes were then fixed and stained with crystal violet. The migrated cells were counted by quantifying the amount of crystal violet using a microscope. Cells were counted in five random fields per well.

### Wound healing assay

To evaluate cell motility, cells ( $1 \times 10^5$  cells/mL) were plated and grown to 80–90% confluency in a six-well plate. After the medium was aspirated, the cell layer was scratched with a 200  $\mu$ L sterile pipette tip and the cells were cultured at 37°C for 48 hours. The average extent of wound closure was monitored and quantified by an Olympus CKX-41 inverted microscope and Olympus E410 camera (Olympus Corporation, Tokyo, Japan). The percent of the wounded area filled with migrating cells was then calculated as follows:  $([\text{mean wound width} - \text{mean remaining width}] / \text{mean wound width}) \times 100$  (%).

### Cell colony formation assay

Cells were trypsinized and suspended in RPMI-1640 medium with 10% calf serum, and 2000 cells/well were seeded into six-well plates in triplicate and cultured at 37°C in a 5% CO<sub>2</sub> incubator for 14 days. Cell colonies were washed with phosphate buffered saline, fixed with methanol for 30 minutes, and stained with crystal violet. Colonies containing ~50 cells were counted, and the mean colony numbers were calculated.

### Cancer stem cell sphere formation assay

Cells were cultured and dissociated into a single-cell suspension and reseeded on six-well ultra-low-attachment plates at a density of  $5 \times 10^3$  cells/well in Dulbecco's modified Eagle medium/F12 medium containing  $1 \times \text{B27}$  supplement, 20 ng/mL epidermal growth factor, and 20 ng/mL basic fibroblast growth factor. The plates were incubated at 37°C in 5% CO<sub>2</sub> for 7 to 10 days to allow CSC sphere formation, followed by qPCR and Western blot analyses.

### In vivo tumorigenesis assay

For the in vivo tumorigenesis assays,  $2 \times 10^6$  L9981 cells with stable linc-ITGB1 knockdown (shlinc-ITGB1) or control cells (shCtrl) were collected and suspended in 0.2 mL of phosphate buffered saline for each mouse (4 in each group, 6–8 weeks old), and the cells were injected into left side of the right flank of BALB/c athymic nude mice. The tumor volumes were calculated using the formula:  $V = (\text{width})^2 \times (\text{length}) \times 0.5$ . The mice were humanely euthanized at the end of the experiments. All animal experiments were performed according to

the National Institutes of Health guidelines on the use of experimental animals.

### Statistical analysis

All experiments were performed independently at least three times. All data are presented as the mean values  $\pm$  standard deviations (SDs) of each group. Statistically significant differences were calculated using a two-tailed Student's *t*-test. The graphs were generated with GraphPad Prism 5.0 (GraphPad, La Jolla, CA, USA).

## Results

### Linc-ITGB1 promotes non-small cell lung cancer (NSCLC) cell stemness

To determine whether linc-ITGB1 could regulate CSC phenotypes of NSCLC, we first detected the expression of linc-ITGB1 in normal adherent cells and stem cell spheres grown in suspension. As depicted in Figure 1a,b, the linc-ITGB1 expression levels were strongly upregulated in L9981 and A549 CSC spheres compared to adherent cells ( $*P < 0.05$ ), and the expression of stemness-associated genes, including *Sox2*, *Nanog*, *Oct-4*, *c-Myc*, and *CD133*, were also significantly higher in CSC spheres ( $*P < 0.05$ ). Upon linc-ITGB1 knockdown, the number of spheres formed by L9981 and A549 cells significantly decreased ( $*P < 0.05$ ) (Fig 1c). Western blot analysis was performed to evaluate the protein levels of the four stemness-associated transcription factors (*Sox2*, *Nanog*, *Oct-4* and *c-Myc*) in spheres, and the results showed that linc-ITGB1 knockdown decreased *Sox2*, *Nanog*, *Oct-4* and *c-Myc* expression levels to varying extents (Fig 1d). Moreover, real-time PCR analysis showed that linc-ITGB1 knockdown markedly decreased the expression of *Sox2*, *Nanog*, *Oct-4*, *c-Myc*, and the cancer stem-associated marker *CD133* ( $*P < 0.05$ ) (Fig 1e,f). These observations suggested that linc-ITGB1 could promote NSCLC cancer stemness by increasing CSC sphere formation and the expression of associated genes.

### Linc-ITGB1 silencing inhibits NSCLC cell proliferation and invasiveness

As CSCs might be responsible for tumor initiation, progression, and invasion because of their capability for self-renewal and potential for proliferation, we investigated the biological functions or roles of linc-ITGB1 in NSCLC cells. The colony formation assay showed that linc-ITGB1 knockdown significantly suppressed L9981 and A549 cell proliferation ( $*P < 0.05$ ) (Fig 2a). To further confirm the role of linc-ITGB1 in tumorigenesis in vivo, NSCLC cells (L9981/shCtrl and L9981/shlinc-ITGB1) were injected into

mice. Tumors formed by L9981/shCtrl cells were obviously larger than those formed by L9981/shlinc-ITGB1 cells ( $*P < 0.05$ ) (Fig 2b), suggesting that linc-ITGB1 could promote tumor growth in vivo.

We then detected the expression of linc-ITGB1 in several human NSCLC cell lines, including two highly metastatic sub-lines (95D and L9981) and their counterparts (95C and NL9980), and two other NSCLC cell lines (A549 and H1299). As depicted in Figure 2c, linc-ITGB1 expression was significantly higher in 95D and L9981 cells than in 95C and NL9980 cells ( $*P < 0.05$ ), indicating that there might be a close correlation between linc-ITGB1 and NSCLC metastasis. A wound healing assay showed a significant reduction in cell migration after linc-ITGB1 knockdown in L9981 and A549 cells ( $*P < 0.05$ ) (Fig 2d), and a transwell assay also indicated that linc-ITGB1 knockdown inhibited L9981 and A549 cell invasion ( $*P < 0.05$ ) (Fig 2e). These data indicated that linc-ITGB1 is involved in the regulation of NSCLC cell metastasis in vitro.

### Linc-ITGB1 promotes epithelial-mesenchymal transition by regulation of Snail expressions in NSCLC cells

The biological function of linc-ITGB1 in inhibiting cell migration and invasion (Fig 2d,e), especially the morphological change from a dispersed and elongated shape to a rounded shape after shlinc-ITGB1 infection (Fig 2f), strongly suggested that linc-ITGB1 regulates EMT in NSCLC cells. We further detected the effect of linc-ITGB1 regulation on EMT-specific biomarkers in L9981 and A549 cells. As indicated by real-time PCR and Western blot (Fig 3a–c), linc-ITGB1 knockdown significantly increased the expression of the epithelial cell marker E-cadherin and decreased the expression of the mesenchymal cell markers vimentin and fibronectin ( $*P < 0.05$ ). These results further confirmed the promoting effect of linc-ITGB1 on EMT progression.

Several transcription factors, including the zinc finger proteins Snail, Slug, Zeb1, Zeb2/SIP1, and Twist, have been implicated in the transcriptional repression of E-cadherin; downregulation of E-cadherin is the hallmark of EMT. Therefore, we used qRT-PCR and Western blot to preliminarily explore whether these transcription factors were involved in the promotion of EMT by linc-ITGB1. As shown in Figure 3d,e, the transcription levels of Snail and Slug were significantly decreased in shlinc-ITGB1-infected cells (L9981 and A549;  $*P < 0.05$ ), while the protein levels of Slug and Twist did not change (Fig 3f). These results implied that linc-ITGB1 regulates EMT mainly by promoting the expression of Snail at both the gene and protein levels. We then transfected shlinc-ITGB1-infected cells with Snail cDNA to observe the effect on EMT markers and found that Snail overexpression reversed the inhibitory effect of shlinc-ITGB1 on EMT by decreasing E-cadherin expression and increasing vimentin

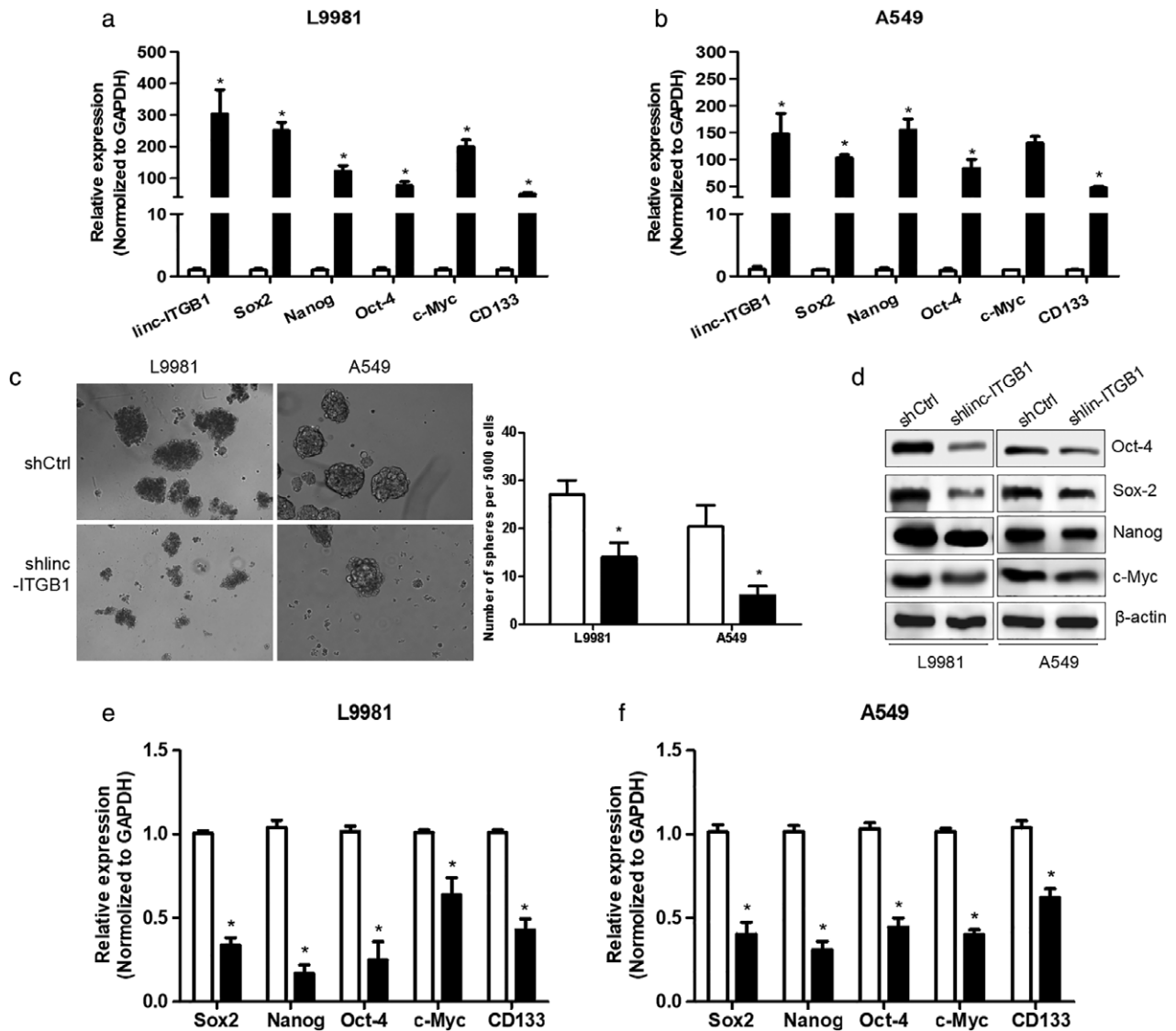


**Figure 1** The effect of linc-ITGB1 depletion on cancer stemness in non-small cell lung cancer cells. Real-time PCR indicated that linc-ITGB1 expression levels were strongly upregulated in (a) L9981. □, Normal; ■, Sphere and (b) A549 cancer stem cell spheres (Sphere) compared to normal adherent cells (Normal) (\* $P < 0.05$ ). □, Normal; ■, Sphere. (c) Linc-ITGB1 knockdown significantly reduced the sphere formation in L9981 and A549 cells, as observed by microscopy (original magnification, 10 $\times$ ) (\* $P < 0.05$ ). □, shCtrl; ■, shlinc-ITGB1. (d) Protein was collected from L9981 and A549 cell spheres for Western blot analysis of the transcription factors Sox2, Nanog, Oct-4, and c-Myc. Real-time PCR was used to detect the expression of stemness-associated genes (Sox2, Nanog, Oct-4, c-Myc, and CD133) in (e) L9981 and (f) A549 cells. □, shCtrl; ■, shlinc-ITGB1. GAPDH, glyceraldehyde 3-phosphate dehydrogenase.

and fibronectin expression in L9981 and A549 cells (\* $P < 0.05$ ) (Fig 3g–i).

### Snail overexpression reverses the inhibitory effect of linc-ITGB1 silencing on NSCLC cancer stemness and invasiveness

Evidence has suggested a strong link between EMT and the CSC metastatic cascade.<sup>18,19</sup> Cells that have undergone EMT can exhibit stem cell properties and stem-like cells

express markers associated with EMT.<sup>18,19</sup> EMT-related transcription factors Snail and Twist are reported to be functionally linked to CSC activation,<sup>20,21</sup> therefore we examined the effect of Snail on NSCLC cell stemness by detecting Snail overexpression in linc-ITGB1 depletion cells. We found that Snail overexpression reversed the inhibitory effect of shlinc-ITGB1 on stemness-associated gene (Sox2, Nanog, Oct-4, c-Myc, and CD133) expression and CSC formation in L9981 cells (\* $P < 0.05$ ) (Fig 4a,b). Wound healing assay indicated that Snail overexpression

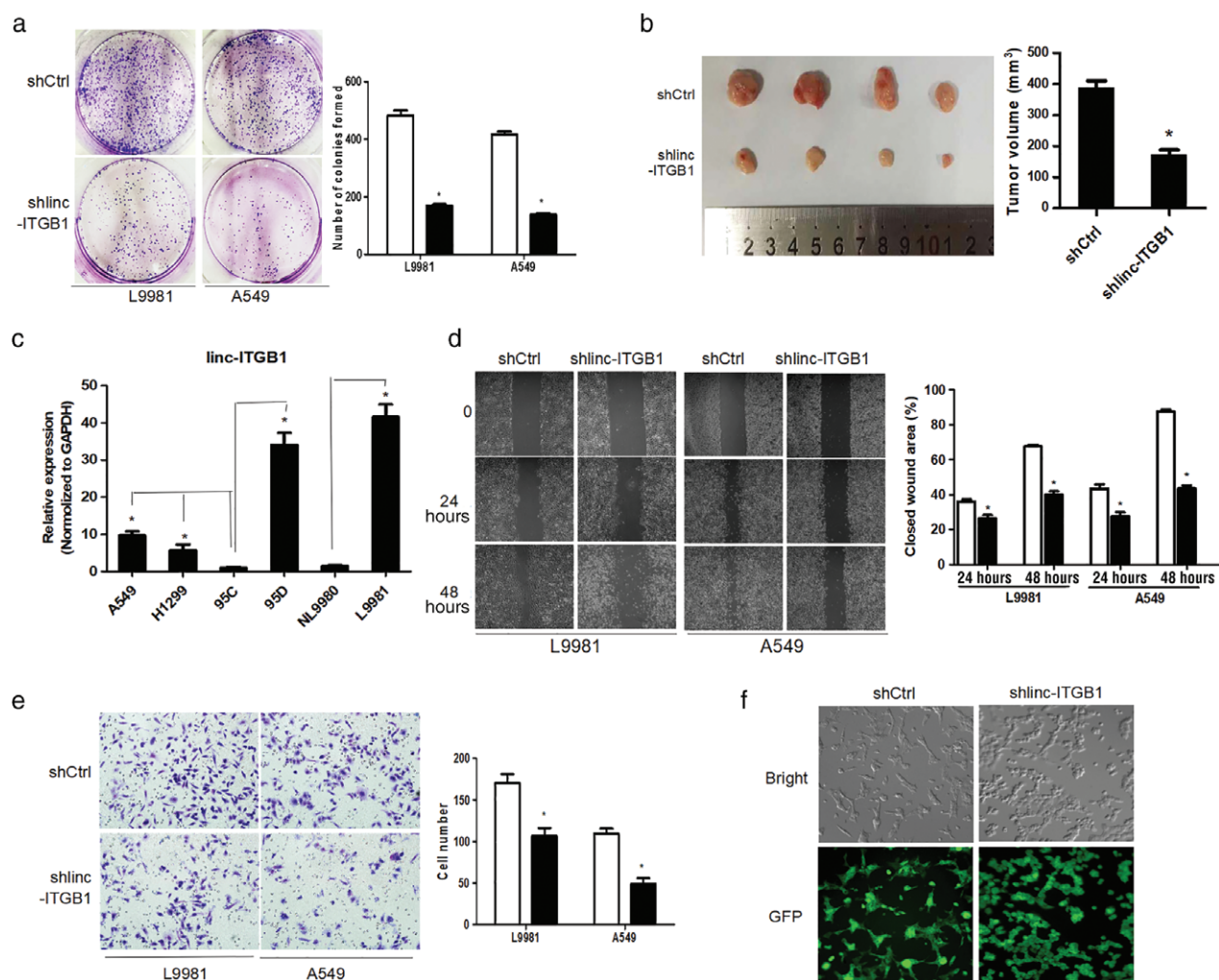


**Figure 2** Linc-ITGB1 silencing inhibits non-small cell lung cancer (NSCLC) cell proliferation and invasiveness. **(a)** Linc-ITGB1 knockdown inhibited colony formation in L9981 and A549 cells, as shown by colony formation assay ( $*P < 0.05$ ). **(b)** Linc-ITGB1 knockdown significantly inhibited the tumor growth of L9981 cells in a nude mouse model. The volume of tumors formed by short hairpin (sh) linc-ITGB1-infected cells was significantly lower than that of tumors formed by shCtrl-infected cells ( $*P < 0.05$ ). **(c)** Relative expression levels of linc-ITGB1 in NSCLC cell lines ( $*P < 0.05$ ). **(d)** Linc-ITGB1 knockdown inhibited cell migration in L9981 and A549 cells, as indicated by wound healing assay ( $*P < 0.05$ ). **(e)** Linc-ITGB1 knockdown inhibited cell invasion in L9981 and A549 cells, as demonstrated by transwell assay ( $*P < 0.05$ ). **(f)** L9981 cells infected with shlinc-ITGB1 for 48 hours were more rounded than shCtrl-infected cells. The cells were visualized by microscopy (original magnification, 20 $\times$ ). GAPDH, glyceraldehyde 3-phosphate dehydrogenase. □, shCtrl; ■, shlinc-ITGB1.

in shlinc-ITGB1-infected L9981 and A549 cells promoted cell migration compared to shlinc-ITGB1-infected cells without Snail overexpression ( $*P < 0.05$ ) (Fig 4c). A transwell invasion assay also showed that Snail cDNA-transfected shlinc-ITGB1-infected cells were more invasive than shlinc-ITGB1-infected cells ( $*P < 0.05$ ) (Fig 4d).

#### Discussion

LncRNAs are increasingly being recognized as playing potential roles in the regulation of tumorigenesis, with aberrant lncRNA expression being found in multiple types of human cancers.<sup>22</sup> LncRNAs could function as key regulators in a wide range of biological processes, including tumor

proliferation, differentiation, apoptosis, and metastasis. In particular, an increasing number of lncRNAs have been found to regulate EMT and cancer stemness by regulating stemness maintaining transcription factors, classic stem cell-related pathways, and relative miRNAs.<sup>23</sup> Linc-ITGB1 was recently shown to be involved in migration and invasion in several types of human cancer;<sup>24</sup> however, the functions and roles of linc-ITGB1 in CSCs have not been reported.

In this study, we found that linc-ITGB1 is significantly upregulated in NSCLC stem cell spheres and highly metastatic NSCLC cell lines, and linc-ITGB1 knockdown inhibited cell proliferation, invasiveness, EMT, and CSC-like properties,

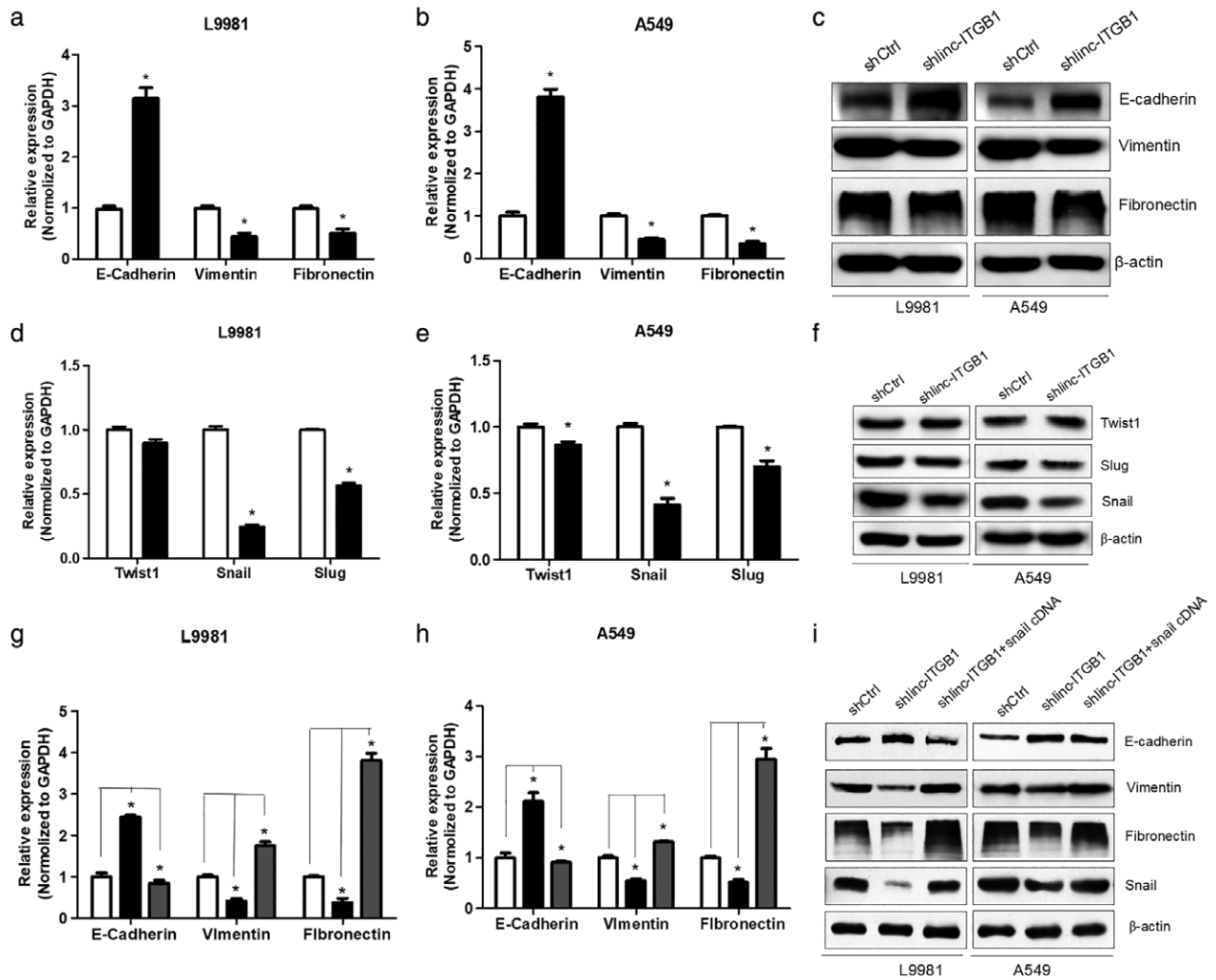


**Figure 3** Linc-ITGB1 depletion inhibited epithelial-mesenchymal transition (EMT) by regulating Snail expression in non-small cell lung cancer (NSCLC) cells. Linc-ITGB1 knockdown significantly induced the expression of E-cadherin and decreased the expression of vimentin and fibronectin in (a) L9981, □, shCtrl; ■, shlinc-ITGB1 and (b) A549 cells, ■, shCtrl, □, shlinc-ITGB1, as determined by real-time (RT) PCR analysis ( $*P < 0.05$ ). (c) Western blots were used to detect the protein levels of E-cadherin, vimentin, and fibronectin;  $\beta$ -actin was used as loading control. ■, shCtrl, ■, shlinc-ITGB1. (d,e) RT-PCR and (f) Western blot analyses of the expression of Twist1, Snail, and Slug in L9981 and A549 cells infected with short hairpin (sh) Ctrl or shlinc-ITGB1 ( $*P < 0.05$ ). (g) L9981 and (h) A549 cells infected with shCtrl or shlinc-ITGB1 alone or cells infected with shlinc-ITGB1 and transfected with Snail complementary DNA were analyzed by RT-PCR to evaluate the transcript levels of the EMT-specific markers E-cadherin, vimentin, and fibronectin ( $*P < 0.05$ ). □, shCtrl, ■, shlinc-ITGB1, ■, shlinc-ITGB1+snailcDNA. (i) Western blot analyses were performed to detect EMT-specific markers in cells treated as indicated in (d) and (e). GAPDH, glyceraldehyde 3-phosphate dehydrogenase.

such as CSC sphere formation and stemness-associated gene expression through the regulation of the transcription factor Snail. Linc-ITGB1 knockdown markedly inhibits the CSC formation and expression of stemness-associated genes, such as *Sox2*, *Nanog*, *Oct-4*, *c-Myc*, and *CD133*. Depletion of linc-ITGB1 expression also inhibits the in vitro invasive and migratory potential of cells, and further analysis indicated that linc-ITGB1 knockdown increases the expression of the epithelial marker E-cadherin and downregulates the mesenchymal markers vimentin and fibronectin. The EMT-related transcription factor Snail mediates these effects of linc-ITGB1

in NSCLC, and overexpression of Snail significantly reverses the inhibitory effects of linc-ITGB1 depletion.

These observations strongly confirm the roles of EMT specific transcription factor Snail in linc-ITGB1 promotion of NSCLC cancer stemness and invasiveness. Therefore, our results suggest that linc-ITGB1 promotes EMT and cancer stemness in NSCLC, mainly via the regulation of Snail expression at both the gene and protein levels; however, the exact molecular mechanism requires further research.

In conclusion, this study provides the first evidence that linc-ITGB1 could promote cancer stemness, EMT, and

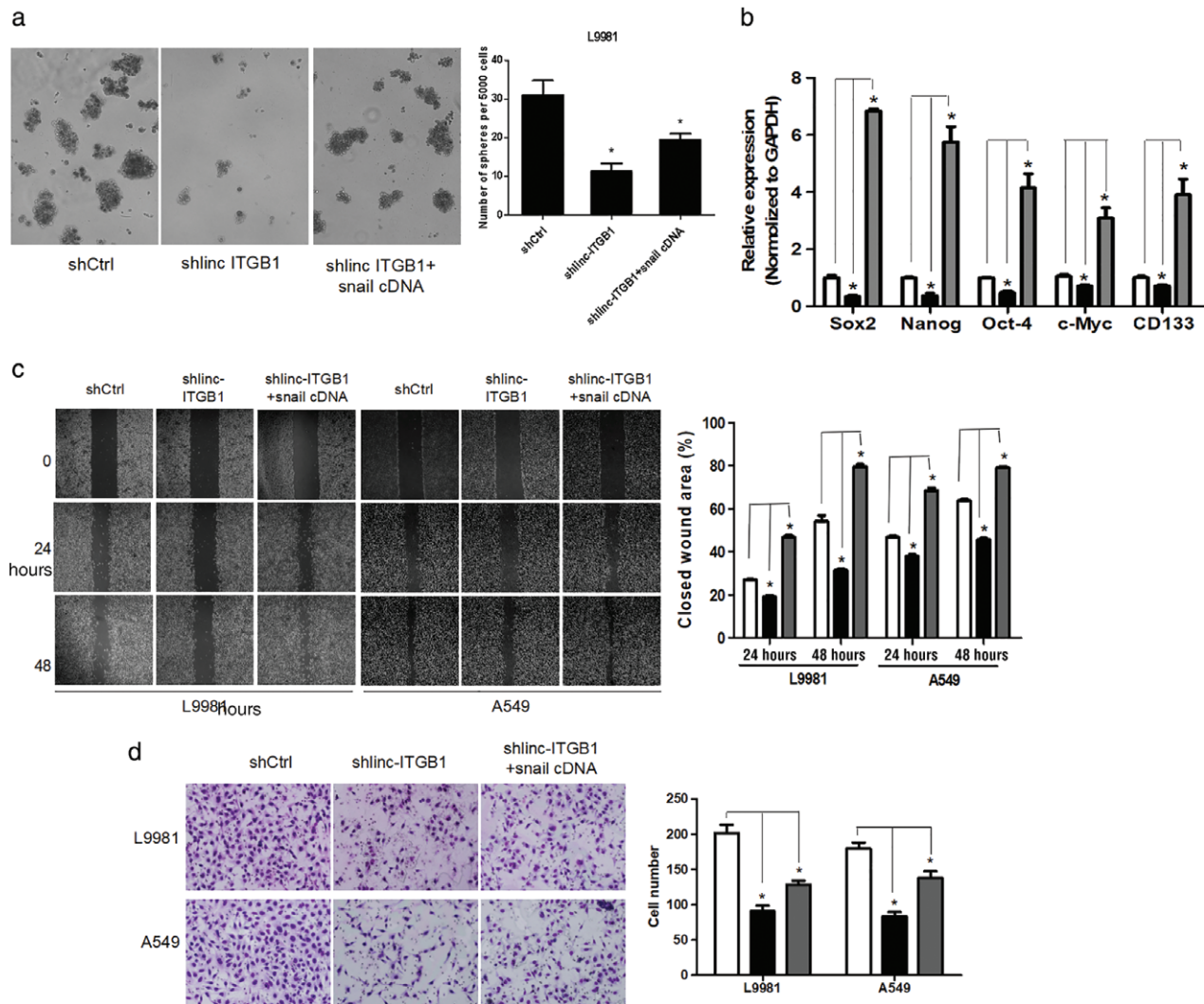


**Figure 4** Snail overexpression reverses the inhibitory effect of linc-ITGB1 depletion on non-small cell lung cancer (NSCLC) stemness and invasiveness. **(a)** Cancer stem cell sphere formation analysis in L9981 cells infected with short hairpin (sh) Ctrl or shlinc-ITGB1 alone or infected with shlinc-ITGB1 and transfected with Snail complementary DNA (cDNA). **(b)** Cells infected with shCtrl or shlinc-ITGB1 alone or cell infected with shlinc-ITGB1 and transfected with Snail complementary DNA were analyzed by RT-PCR to evaluate the transcript levels of the stemness-associated gene (Sox-2, Nanog, Oct-4, c-Myc and CD133) expression. **(c)** The migration ability of L9981 and A549 cells infected with shCtrl or shlinc-ITGB1 alone or infected with shlinc-ITGB1 and transfected with Snail cDNA was analyzed by wound healing assay ( $*P < 0.05$ ). □, shCtrl, ■, shlinc-ITGB1, ▨, shlinc-ITGB1+snailcDNA. **(d)** The invasion ability of cells infected with shCtrl or shlinc-ITGB1 alone or infected with shlinc-ITGB1 and transfected with Snail cDNA was analyzed by a transwell experiment ( $*P < 0.05$ ). □, shCtrl, ■, shlinc-ITGB1, ▨, shlinc-ITGB1+snailcDNA. GAPDH, glyceraldehyde 3-phosphate dehydrogenase.

proliferation in NSCLC through regulation of the transcription factor Snail. These data indicate that linc-ITGB1 might be a potential promoting factor in lung cancer metastasis, and further investigation is needed to elucidate the exact molecular pathways regulated by linc-ITGB1.

## Acknowledgments

This study was supported by grants from the National Natural Science Foundation of China (No.81702267).

## Disclosure

No authors report any conflict of interest.

## References

- 1 Ferlay J, Soerjomataram I, Dikshit R *et al.* Cancer incidence and mortality worldwide: Sources, methods and major patterns in GLOBOCAN 2012. *Int J Cancer* 2015; **136**: e359–86.
- 2 Al-Hajj M, Wicha MS, Benito-Hernandez A, Morrison SJ, Clarke MF. Prospective identification of tumorigenic breast cancer cells. *Proc Natl Acad Sci U S A* 2003; **100**: 3983–8.



- 3 Easwaran H, Tsai HC, Baylin SB. Cancer epigenetics: Tumor heterogeneity, plasticity of stem-like states, and drug resistance. *Mol Cell* 2014; **54**: 716–27.
- 4 Scheel C, Weinberg RA. Cancer stem cells and epithelial-mesenchymal transition: Concepts and molecular links. *Semin Cancer Biol* 2012; **22**: 396–403.
- 5 Yeung KT, Yang J. Epithelial-mesenchymal transition in tumor metastasis. *Mol Oncol* 2017; **11**: 28–39.
- 6 Tam WL, Weinberg RA. The epigenetics of epithelial-mesenchymal plasticity in cancer. *Nat Med* 2013; **19**: 1438–49.
- 7 Nieto MA, Huang RY, Jackson RA, Thiery JP. Emt: 2016. *Cell* 2016; **166**: 21–45.
- 8 Rodríguez-Mateo C, Torres B, Gutiérrez G, Pintor-Toro JA. Downregulation of Lnc-Spry1 mediates TGF-beta-induced epithelial-mesenchymal transition by transcriptional and posttranscriptional regulatory mechanisms. *Cell Death Differ* 2017; **24**: 785–97.
- 9 Bhan A, Soleimani M, Mandal SS. Long noncoding RNA and cancer: A new paradigm. *Cancer Res* 2017; **77**: 3965–81.
- 10 Liu A, Liu S. Noncoding RNAs in growth and death of cancer cells. *Adv Exp Med Biol* 2016; **927**: 137–72.
- 11 Ying L, Chen Q, Wang Y, Zhou Z, Huang Y, Qiu F. Upregulated MALAT-1 contributes to bladder cancer cell migration by inducing epithelial-to-mesenchymal transition. *Mol Biosyst* 2012; **8**: 2289–94.
- 12 Luo M, Li Z, Wang W, Zeng Y, Liu Z, Qiu J. Long non-coding RNA H19 increases bladder cancer metastasis by associating with EZH2 and inhibiting E-cadherin expression. *Cancer Lett* 2013; **333**: 213–21.
- 13 Wei S, Wang K. Long noncoding RNAs: Pivotal regulators in acute myeloid leukemia. *Exp Hematol Oncol* 2016; **5**: 30.
- 14 Gupta RA, Shah N, Wang KC *et al.* Long non-coding RNA HOTAIR reprograms chromatin state to promote cancer metastasis. *Nature* 2010; **464**: 1071–6.
- 15 He W, Cai Q, Sun F *et al.* linc-UBC1 physically associates with polycomb repressive complex 2 (PRC2) and acts as a negative prognostic factor for lymph node metastasis and survival in bladder cancer. *Biochim Biophys Acta* 2013; **1832**: 1528–37.
- 16 Wang L, Zhang Y, Lv W *et al.* Long non-coding RNA Linc-ITGB1 knockdown inhibits cell migration and invasion in GBC-SD/M and GBC-SD gallbladder cancer cell lines. *Chem Biol Drug Des* 2015; **86**: 1064–71.
- 17 Yan M, Zhang L, Li G, Xiao S, Dai J, Cen X. Long noncoding RNA linc-ITGB1 promotes cell migration and invasion in human breast cancer. *Biotechnol Appl Biochem* 2017; **64**: 5–13.
- 18 Mani SA, Guo W, Liao MJ *et al.* The epithelial-mesenchymal transition generates cells with properties of stem cells. *Cell* 2008; **133**: 704–15.
- 19 Dima M, Pecce V, Biffoni M *et al.* Molecular profiles of cancer stem-like cell populations in aggressive thyroid cancers. *Endocrine* 2016; **53**: 145–56.
- 20 Lamouille S, Xu J, Derynck R. Molecular mechanisms of epithelial-mesenchymal transition. *Nat Rev Mol Cell Biol* 2014; **15**: 178–96.
- 21 Zheng X, Carstens JL, Kim J *et al.* Epithelial-to-mesenchymal transition is dispensable for metastasis but induces chemoresistance in pancreatic cancer. *Nature* 2015; **527**: 525–30.
- 22 Gibb EA1, Brown CJ, Lam WL. The functional role of long non-coding RNA in human carcinomas. *Mol Cancer* 2011; **10**: 38.
- 23 Yan H, Bu P. Non-coding RNAs in cancer stem cells. *Cancer Lett* 2018; **421**: 121–6.
- 24 Shang M, Xu X, Zhang M, Yang H. Long non-coding RNA linc-ITGB1 promotes cell proliferation and migration in human hepatocellular carcinoma cells. *Exp Ther Med* 2017; **14**: 4687–92.